12th IFAC International Symposium on
Advanced Control of Chemical Processes
July 14-17, 2024. Toronto, Canada

Self-Stabilizing Economic Nonlinear Model Predictive Control for Membrane Reactors

San Dinh, **Lorenz T. Biegler** *

* *Carnegie Mellon University, Pittsburgh, PA 15213 USA (e-mail: lb01@andrew.cmu.edu)*

Abstract: The paper extends recent advancements in self-stabilizing eNMPC formulation without pre-calculated setpoints, which leverages norm-based steady-state optimality conditions to enhance system robustness. To facilitate practical implementation, a generalized time-domain formulation is proposed, accommodating the discrete-time nature of control instrumentation and the continuous-time nature of first-principle models. The online computational time of the self-stabilizing eNMPC is improved via the simplification of the Lyapunov function. A case study involving a modular membrane reactor illustrates the applicability of self-stabilizing eNMPC in real-world industrial scenarios.

Keywords: Economic Nonlinear Model Predictive Control, Lyapunov Stability, Self-Stabilization, Input-to-State Practical Stability, Pyomo

1. INTRODUCTION

Economic Nonlinear Model Predictive Control (eNMPC) represents a viable alternative to a distributed control system for addressing the challenges that arise from the mismatch between Real-Time Optimizers (RTO) and Model Predictive Controllers (MPC). Standard eNMPC is formulated as a nonlinear programming (NLP) problem that combines the economic objective function of RTO with the dynamic prediction of MPC. While eNMPC offers significant advantages, it also introduces challenges related to closed-loop stability (Angeli et al., 2012).

In recent times, a self-stabilizing eNMPC without pre-calculated steady-state optima was proposed by replacing the tracking stage cost with a norm of the steady-state optimality conditions (Karush–Kuhn–Tucker or KKT conditions) (Lin and Biegler, 2023). While the theoretical framework that underpins the self-stabilizing eNMPC demonstrates robustness, there is an imperative need for a comprehensive and pragmatic implementation strategy. In this work, the primary objective revolves around the adaptation of the existing self-stabilizing eNMPC framework for practical implementation. This adaptation aims to facilitate smooth integration with well-established algebraic modeling platforms, such as Pyomo, AVEVA, or Aspen Custom Modeler, which are commonly employed for describing chemical processes.

A case study on a modular membrane reactor for direct methane aromatization (DMA-MR) is conducted to illustrate the practical application of self-stabilizing eNMPC. A modular process is a self-contained system built within a frame or "module" for easy transportation and integration (Baldea et al., 2017). This system encompasses process equipment, instrumentation, valves, piping components, and electrical wiring, all securely mounted within a structural steel framework (Ladiges et al., 2018). Given the autonomous nature of modular units, employing a self-stabilizing eNMPC emerges as an ideal choice for the integrated control system.

The paper is organized as follows in the subsequent sections, with the aim of identifying any encountered limitations and offering recommendations for further exploration and refinement of the proposed control system within industrial contexts. Section 2 introduces foundational knowledge on eNMPC and provides a mathematical description of dynamic processes in continuous and discrete time domains. In Section 3, the formulation of self-stabilizing eNMPC is presented, along with modifications aimed at enhancing the rate of convergence to steady-state optima and the online solution strategy for the controller. A case study is presented in Section 4, which includes a first-principles dynamic model for a counter-current DMA-MR and its self-stabilizing eNMPC simulations. Finally, Section 5 concludes the paper by summarizing the key takeaways and emphasizing the broader implications of these findings.

2. PROCESS DESCRIPTIONS

2.1 Notations

In the scope of this investigation, the following notations are taken into consideration. A function denoted as $\alpha(\xi) : \mathbb{R}\geq 0 \to \mathbb{R}\geq 0$ is classified as a member of the $\mathcal{K}$ function class if it exhibits the properties of continuity, strict monotonicity, and $\alpha(0) = 0$. A function α falls within the $\mathcal{K}_\infty$ class if it is in the $\mathcal{K}$ class and is unbounded. The L^2-norm of a vector is symbolized by $\|\cdot\|$. The metric defining the distance between a point $x \in \mathbb{R}^{n_x}$ and a set $A \subset \mathbb{R}^{n_x}$ is formulated as $\|x\|_A := \inf_{z\in A} \|x - z\|$. If the set $A = \{x^*\}$ only contains a single point, then $\|x\|_A := \|x - x^*\|$ and $\lim_{x\to x^*} \|x\|_A = 0$. A closed set A is a positive invariant set for a closed-loop discrete-time system $x_{k+1} = \bar{f}(x_k, u_k) = \bar{f}(x_k, \kappa(x_k))$ if $x_k \in A$ implies $x_{k+1} \in A$.

2.2 System Description

The first-principles dynamic model is assumed to be represented by a system of semi-explicit differential-algebraic equations of index-1, and it is expressed in a nonlinear state-space structure as follows.

$$\dot{x}(t) = f(x(t), y(t), u(t)) \tag{1a}$$
$$h(x(t), y(t), u(t)) = 0 \tag{1b}$$
$$g(x(t), y(t), u(t)) \leq 0 \tag{1c}$$

in which for each time instance t, $x(t) \in \mathbb{R}^{n_x}$ is the vector of state variables, $\dot{x}(t) \in \mathbb{R}^{n_x}$ is the time derivative vector of state variables, $y(t) \in \mathbb{R}^{n_y}$ is a vector of algebraic variables (for which no time derivatives are present), $u(t) \in \mathbb{R}^{n_u}$ is the vector of manipulated variables. The rate of change equations, $f : \mathbb{R}^{n_x+n_y+n_u} \to \mathbb{R}^{n_x}$, reflect the process dynamics. In engineering applications, the algebraic equations $h : \mathbb{R}^{n_x+n_y+n_u} \to \mathbb{R}^{n_h}$ encompass various aspects of the systems under consideration, including equilibrium conditions, relationships among different variables and equality constraints.

For a fixed sampling period, Δt, the following time index conversion is introduced between a continuous-time dynamic system and a discrete-time dynamic system.

$$t_k = k\Delta t \tag{2}$$

For ease of notation, the discrete-time vectors of state variables, algebraic variables, and manipulated variables are respectively denoted as $x_k = x(t_k)$, $y_k = y(t_k)$, and $u_k = u(t_k)$. The discrete-time dynamic model of the above system in (1) is:

$$x_{k+1} = \bar{f}\left(x_k, y_k, u_k\right) = x_k + \int_{t_k}^{t_{k+1}} f(x(t), y(t), u(t))dt \tag{3a}$$
$$h(x_k, y_k, u_k) = 0 \tag{3b}$$
$$g\left(x_k, y_k, u_k\right) \leq 0 \tag{3c}$$

In this context, $\bar{f}$ represents the time-discretized version of the dynamic model (1), incorporating a zero-order hold on the manipulated variables.

2.3 Economic Nonlinear Model Predictive Control

Economic Nonlinear Model Predictive Control presents a dynamic programming problem that integrates economic process optimization with the principles of model predictive control. In the eNMPC formulation, the setpoint-tracking objective function of MPC is replaced by a cost function that combines process performance objectives with financial considerations. Additionally, a nonlinear dynamic model is embedded within the constraints to delineate feasible operating regions. The standard eNMPC is characterized by the following optimization problem.

$$\min \quad \sum_{l=0}^{N-1} \Psi^{ec}\left(s_l, w_l, v_l\right) \tag{4a}$$
$$\text{s.t.} \quad s_{l+1} = \bar{f}\left(s_l, w_l, v_l\right), \quad l = 0, \dots N-1 \tag{4b}$$
$$h(s_l, w_l, v_l) = 0 \tag{4c}$$
$$g(s_l, w_l, v_l) \leq 0 \tag{4d}$$
$$s_0 = x_k \tag{4e}$$

in which, the economic stage cost, Ψ^{ec}, represents economic factors, such as production costs, resource utilization, energy consumption, profit margins, or other relevant financial metrics to the specific application. The triplet (s, w, v) is the respective prediction of the real process variables (x, y, u). At each time step t_k, the nonlinear optimizer of the eNMPC receives the estimated state variables, x_k, and assigns them to the initial conditions, as demonstrated in constraint (4e).

3. IMPLEMENTATION OF SELF-STABILIZING ENMPC

3.1 Steady-State Optimality Conditions

The following steady-state optimization problem is considered for the RTO in order to identify the KKT condition for the self-stabilizing Lyapunov function.

$$\min_{x,u} \quad \Psi^{ec}(x, u, y) \tag{5a}$$
$$\text{s.t.} \quad x = \bar{f}\left(x, u, y\right) \tag{5b}$$
$$h\left(x, u, y\right) = 0 \tag{5c}$$
$$g\left(x, u, y\right) \leq 0 \tag{5d}$$

The log-barrier function is a powerful tool in optimization that enables the handling of inequality constraints without the need for active set strategies. In the following reformulation of (5), the inequalities in (5d) are replaced by their respective barrier functions.

$$\min_{x,u} \quad \bar{\Psi}^{ec}(x, u, y) := \Psi^{\mathrm{ec}}(x, u, y) - \mu \sum_{j=1}^{n_g} \ln\left(-g_j(x, u, y)\right) \tag{6a}$$
$$\text{s.t.} \quad 0 = F(x, y, u) = \begin{bmatrix} x - \bar{f}(x, y, u) \\ h(x, y, u) \end{bmatrix} \tag{6b}$$

in which the $\bar{\Psi}^{ec}$ is the augmented steady-state objective, $\mu > 0$ is the barrier parameter, and n_g is the number of inequality constraints. Since the log-barrier function approaches infinity when an inequality constraint becomes active, the value of μ is chosen to be very small to allow the optimal solution of (6) to converge to the optimal solution of (5). This modification in Problem (6) is borrowed from the interior point method for solving constrained optimization problems.

Since the self-stabilizing eNMPC discussed in the following section penalizes deviation from the steady-state optimal condition rather than the distance from the steady-state optimal solution, this objective revision results in a KKT condition that incorporates the complementary property of the KKT multipliers associated with the inequalities. Furthermore, this KKT condition facilitates a smooth transition between active and inactive inequality constraints, thus making it a suitable choice for inclusion into the Lyapunov function. The Lagrangian of (6) is as follows.

$$L(x, y, u, \lambda) = \bar{\Psi}^{ec}(x, y, u) + F(x, y, u)^{\intercal}\lambda \tag{7}$$

in which λ is the Lagrange multiplier of the steady-state equalities.

The following KKT conditions are the first-order necessary conditions for a steady-state optimum of (6) (Nocedal and Wright (2006)).

$$\nabla_x L = \nabla_x \bar{\Psi}^{ec}(x,y,u) + \nabla_x F(x,y,u)\lambda = 0 \quad (8a)$$
$$\nabla_y L = \nabla_y \bar{\Psi}^{ec}(x,y,u) + \nabla_y F(x,y,u)\lambda = 0 \quad (8b)$$
$$\nabla_u L = \nabla_u \Psi^{ec}(x,y,u) = 0 \quad (8c)$$
$$\nabla_\lambda L = F(x,y,u) = 0 \quad (8d)$$

Furthermore, the steady-state system is assumed to satisfy the Strong Second Order Sufficient Conditions (SSOSC) and Linear Independent Constraint Qualification (LICQ) (Nocedal and Wright, 2006). These assumptions guarantee that the KKT conditions in (8) are sufficient to identify the steady-state optimum of (6) and subsequently (5).

3.2 Generalized-Time Formulation of Self-stabilizing eNMPC

The foundation of Lyapunov stability theory rests on the notion of energy dissipation and its relationship to the stability of dynamical systems. Here, a Lyapunov function can be linked to a mathematical emulation of potential energy. This function assigns a scalar value to every state within the system, thereby representing and quantifying the system's pseudo-energy associated with that particular state. Formally, the Lyapunov function is defined as follows.

Definition 1. A Lyapunov function, $V : \mathbb{R}^{n_x} \to \mathbb{R}_{\geq 0}$ exists for the discrete-time dynamic system, $x_{k+1} = \bar{f}(x_k, \kappa(x_k))$ with respect to a positive invariant set A if $\bar{f}$ is locally bounded, and there exist functions α_1, α_2 of class $\mathcal{K}_\infty$, and a positive definite function ϕ_d that satisfy the following:

$$\alpha_1(\|x\|_A) \leq V(x) \leq \alpha_2(\|x\|_A) \quad (9)$$
$$V(\bar{f}(x,\kappa(x))) - V(x) \leq -\phi_d(\|x\|_A) \quad (10)$$

The existence of a Lyapunov function implies asymptotic convergence to a set A, and it is well-known as the Lyapunov theorem (Rawlings et al., 2020). Typically, inequalities (9) and (10) are incorporated into the constraints of a standard eNMPC to achieve stabilization, with the Lyapunov function selected from the tracking stage cost. This choice aligns with setting A as the steady-state optimal setpoint, and the distance from the set A is the norm of the difference from the setpoint.

The rationale behind a self-stabilizing Lyapunov constraint for eNMPC in the absence of a precomputed steady-state lies in the notion of penalizing deviations from the steady-state conditions rather than penalizing differences from the steady-state optimal solution. In short, the set A in self-stabilizing eNMPC is determined by the norm of the KKT conditions, as presented in equation (8). This, in turn, leads to the subsequent formulation of the stage cost and Lyapunov function.

$$\begin{aligned}\Psi^{tr}(s_l, w_l, v_l, \lambda^*) := {} & \|F(s_l, w_l, v_l)\|^2 \\ & + \|\nabla_s L(s_l, w_l, v_l, \lambda^*)\|^2 \\ & + \|\nabla_w L(s_l, w_l, v_l, \lambda^*)\|^2 \\ & + \|\nabla_v L(s_l, w_l, v_l, \lambda^*)\|^2\end{aligned} \quad (11)$$

$$V(x_k) := \sum_{l=0}^{N-1} \Psi^{tr}(s_l, w_l, v_l,\ \lambda^*) \quad (12)$$

where $\Psi^{tr}(s_l, w_l, v_l, \lambda^*)$ is the stage cost at predictive time l, λ^* is defined from (13g) and $V(x_k)$ is the Lyapunov function at operating time k. This distinction of index signifies the roles of the predictive variables s_l and the actual variables x_k in the controller. The values of the triplet (s_l, w_l, v_l) are calculated according to the current states x_k for all values of l in the predictive horizon. Thus, while sharing the same notations, the values of (s_l, w_l, v_l) in the expression of $V(x_k)$ and those in the expression of $V(x_{k+1})$ take different values, as they represent solutions to two distinct constrained optimization problems.

In the formulation of the self-stabilizing eNMPC, the augmented components of the stage cost and the Lyapunov function, as delineated previously, are incorporated into the standard eNMPC framework. Specifically, at discrete time instances denoted as t_k, the subsequent constrained optimization problem is solved to achieve the optimal control actions.

$$\min \sum_{l=0}^{N-1} \Psi^{ec}(s_l, w_l, v_l) \quad (13a)$$
$$\text{s.t.} \quad s_{l+1} = \bar{f}(s_l, w_l, v_l), \quad l = 0, \dots N-1 \quad (13b)$$
$$h(s_l, w_l, v_l) = 0 \quad (13c)$$
$$g(s_l, w_l, v_l) \leq 0 \quad (13d)$$
$$s_0 = x(t_k) \quad (13e)$$
$$V(x_k) \leq V(x_{k-1}) - \Psi^{tr}(x_{k-1}, u_{k-1}) \quad (13f)$$
$$\nabla_s L(s_N, w_N, v_N, \lambda^*) = 0 \quad (13g)$$
$$\nabla_w L(s_N, w_N, v_N, \lambda^*) = 0 \quad (13h)$$
$$\nabla_v L(s_N, w_N, v_N, \lambda^*) = 0 \quad (13i)$$
$$F(s_N, w_N, v_N) = 0 \quad (13j)$$

The values of (s_l, w_l, v_l) are conditional on the initialization of s_0 with an estimation of x_k. Thus, the right-hand side of the Lyapunov constraint (13f) is taken from the solution of the eNMPC in the previous time step t_{k-1}, and it is a constant value at the current time t_k.

In the eNMPC formulation (13), the steady-state KKT conditions are exclusively incorporated into the endpoint constraints of the predictive horizon, and there are dual intentions for this substitution. Firstly, the Lagrange multiplier is not defined by index l; instead λ^* is set to be the same for all stage costs in the predictive horizon. This approach was proposed in Lin and Biegler (2023), where it is proved to guarantee the asymptotic stability of a closed-loop system. Consequently, the Lagrange multipliers are recalculated only in the event of a parameter update. Otherwise, these multipliers remain constant to reduce the computational time of the eNMPC.

3.3 Rate of Convergence Modification

Although the self-stabilizing eNMPC described in (13) can guide the dynamic process towards the optimal steady state without relying on pre-calculated setpoints, managing the rate of convergence to this steady state can be advantageous during online operation. For instance, in cases where cyclic optimal behaviors are observed, and it is economically advantageous for the process to operate in a transient state rather than maintaining a steady state, decreasing the rate of convergence can be beneficial to capture short-term gains. Conversely, if the process is more cost-effective at the new steady state, eNMPC should expedite the process toward achieving the optimal steady-state condition. In order to achieve more control over the rate of convergence, the Lyapunov constraint (13f) is modified as follows.

$$V(x_k) \leq (1-\delta_1)V(x_{k-1}) - \delta_2 \Psi^{tr}(x_{k-1}, u_{k-1}) \tag{14}$$

in which, $\delta_1 \in [0, 1)$ and $\delta_2 \in (0, 1]$. When δ_1 is set to zero, the Lyapunov constraint (14) becomes identical to the previously proposed Lyapunov constraint in self-stabilizing eNMPC(Lin and Biegler, 2023), ensuring robust stability. Since δ_1 is strictly less than 1, the positive definite Lyapunov function $V(x_{k-1})$ causes the constraint (14) to be strictly less than its right-hand side with $\delta_1 = 0$. Thus, the incorporation of additional tuning parameters maintains the robust stability of the previously established formulation.

Furthermore, the right-hand side of (14) is bounded above by $(1-\delta_1)V(x_{k-1})$. Thus, the closed-loop process converges to the optimal steady-state at an exponential rate $(1-\delta_1)^k V(x_0)$ as follows.

$$\begin{aligned} V(x_k) &\leq (1-\delta_1)V(x_{k-1}) - \delta_2 \Psi^{tr}(x_{k-1}, u_{k-1}) \\ &\leq (1-\delta_1)V(x_{k-1}) \leq (1-\delta_1)^2 V(x_{k-2}) \\ &\leq \ldots \leq (1-\delta_1)^k V(x_0) \end{aligned} \tag{15}$$

3.4 Online Solution Strategy

Our eNMPC formulation is implemented within the Pyomo algebraic modeling environment, as an efficient framework for online computation. This framework deliberately initializes the nonlinear program using the recently developed built-in Dynamic Interface (Parker et al., 2023). Given that eNMPC inherits the predictive characteristics of MPC, it is noteworthy that the optimal control actions for two consecutive time steps should not differ significantly from each other, especially when the predictive horizon is sufficiently long. Therefore, a strategic initialization scheme for the current time step is constructed by shifting the predictions from the previous eNMPC solution backward by one time step. While this strategy is applicable across various modeling environments, the Dynamic Interface in Pyomo simplifies this task substantially by reorganizing the block-hierarchical structure within the model solution. When dealing with model variables stored using a complex index structure, this interface can effectively slice and sort the variable data into time-indexed snapshots, facilitating the extraction and shifting of instances for the initialization of the subsequent time step.

4. CASE STUDY: DIRECT METHANE AROMATIZATION

In this work, a dynamic model of a counter-current membrane reactor for Direct Methane Aromatization (DMA-MR) is constructed. While a counter-current membrane reactor has proved to have higher conversion rates in other intensified processes (Bishop and Lima, 2021), it has not been previously investigated for the DMA-MR. A schematic of the counter-current flow configuration of the DMA-MR is provided in Figure 1. The dynamic model of the DMA-MR is assumed to operate under rigorous temperature and pressure control, maintaining both isothermal and isobaric conditions throughout its operation. Within this framework, the influence of pressure drops is deliberately omitted, and emphasis is placed on

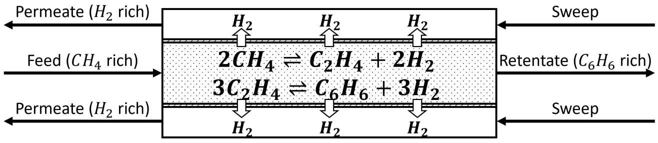

Fig. 1. Schematic with inputs, outputs, and reactions of the DMA-MR

the impact of pressure profiles within the tube and shell on the flow rate. This simplification allows for the assumption of a 1-dimensional model with no radial profile, effectively reducing the complexity of the analysis to variations in states along the DMA-MR's length. The ideal gas law is selected to describe the gas behavior within the system. The method of lines discretization is applied along the length of the reactor to convert it into a system of differential-algebraic equations. Additional details of the dynamic DMA-MR model can be found in Dinh et al. (2024).

4.1 Closed-Loop Simulation

In the context of closed-loop simulations for eNMPC, an economic stage cost is employed to minimize downstream separation costs for the permeate and retentate, which are assumed to be proportional to their respective flow rates. The economic objective is also to maximize the production of both benzene in the tube as well as hydrogen in the shell. The formulation for the stage cost at time k is as follows:

$$\begin{aligned} \Psi^{ec} = &-(\phi_{C_6H_6} C_{t,C_6H_6}(L,k) - \phi_{tube}) Q_{tube,k} \\ &-(\phi_{H_2} C_{s,H_2}(0,k) - \phi_{shell}) Q_{shell,k} \end{aligned} \tag{16}$$

in which at every discrete time k, $Q_{tube,k}$ is the volumetric flow rate of the tube inlet, $Q_{shell,k}$ is the volumetric flow rate of the shell inlet, $\phi_{C_6H_6}$ denotes the profit from producing C_6H_6, ϕ_{H_2} denotes the profit from producing H_2, ϕ_{tube} denotes the separation cost of the permeate, and ϕ_{shell} denotes the separation cost of the retentate. It is important to note that the main focus of the case study is to demonstrate the application of self-stabilizing eNMPC to DMA-MR, rather than provide techno-economic analysis of its operation. Thus, Ψ^{ec} in (16) is dimensionless, and its quantitative values serve as evaluations of eNMPC performance instead of actual operating cost. Furthermore, the function Ψ^{ec} in (16) is not a $\mathcal{K}$ class function, so the closed-loop stability of a standard eNMPC (4) is not guaranteed without a stabilizing constraint.

In the first scenario, the application of self-stabilizing eNMPC to a system with parameter updates serves to illustrate its capacity to achieve convergence to steady-state optima without relying on predefined setpoints. The simulation results for this scenario are illustrated in Figure 2. The closed-loop system demonstrates its convergence to the initial steady state by the 62$^{\text{nd}}$ time step. Subsequently, at the 100$^{\text{th}}$ time step, a modification is introduced in the boundary condition of the tube inlet, transitioning it from 95% methane to 85% methane. Notably, the proposed eNMPC framework effectively guides the system to a new steady-state optimum by the 169$^{\text{th}}$ time step, all without the necessity of pre-established setpoints. This demonstration underscores that the dynamic system can be systematically directed toward the respective steady-state solutions through the indirect penalization of the

Lyapunov function with the norm of the steady-state KKT conditions.

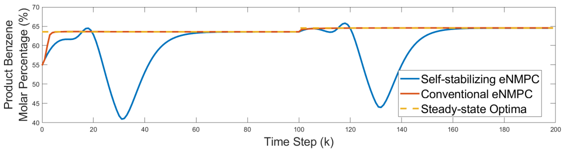

(a) Output variable: benzene molar percentage in retentate

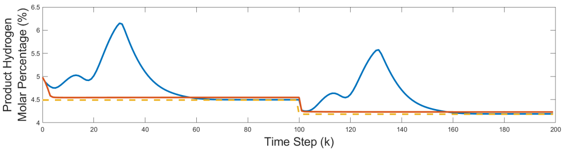

(b) Output variable: hydrogen molar percentage in permeate

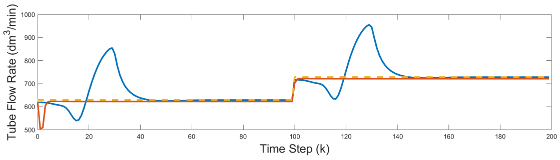

(c) Manipulated variable: inlet volumetric flow rate in tube side

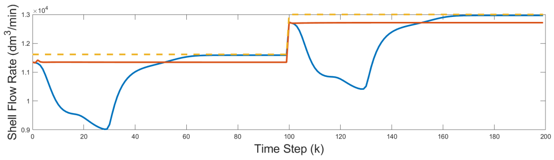

(d) Manipulated variable: inlet volumetric flow rate in shell side

Fig. 2. Self-stabilizing eNMPC convergence to new steady-state optima without pre-calculated setpoints

In this case study, we explore three distinct online solution approaches: i) formulation of *alternative KKT tracking stage cost with fixed multipliers* (λ^*) from the solution of (5), ii) *alternative KKT tracking stage cost with free* λ^*, which are determined in (13) and iii) *full KKT tracking stage cost* derived in Lin and Biegler (2023), which integrates the stage cost (11) and Lyapunov function (12) into the stabilizing and terminal constraints of (13). This approach requires recomputation of Lagrange multipliers at each predictive time step. A computational time comparison in Figure 3 reveals superior efficiency of alternative KKT tracking formulations, despite the slightly longer computational time of the *alternative KKT tracking stage cost with free multipliers*. Overall, these approaches exhibit similar trends, with two peaks in computational time following setpoint changes in self-stabilizing eNMPC, reflecting adjustments in Lagrange multipliers to track new steady-state optima and align predictive trajectories.

In the subsequent scenario within the case study, an adjustment is made to the tuning parameters specified in (14) to illustrate their impact on the convergence rate to steady-state optima. Given that both δ_1 and δ_2 exert a monotonic influence on the convergence rate, it is appropriate to simplify the analysis by selecting the values for these parameters as $\delta = \delta_2 = 2\delta_1$. The simulations with varying values of δ are shown in Figure 4. From these results, it is observed that the time required to reach steady state shortens as $\delta \to 1$, while it lengthens as this parameter decreases. Moreover, for the case where

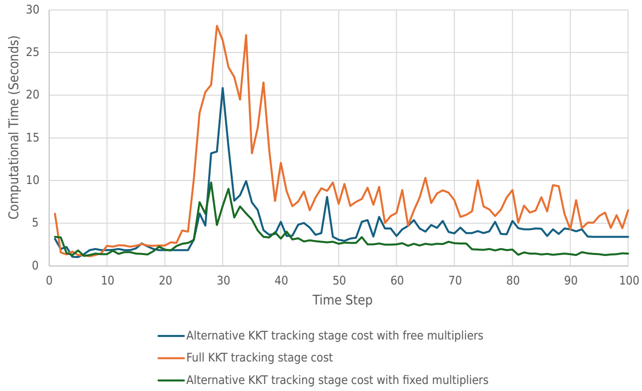

Fig. 3. Online computational time for the self-stabilizing eNMPC with parameter update

$\delta = 1$, the economic performance is improved by 24% over standard eNMPC.

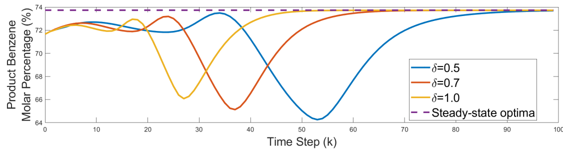

(a) Output variable: benzene molar percentage in retentate

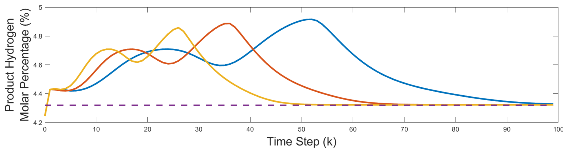

(b) Output variable: hydrogen molar percentage in permeate

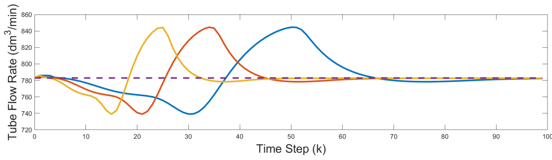

(c) Manipulated variable: inlet volumetric flow rate in tube side

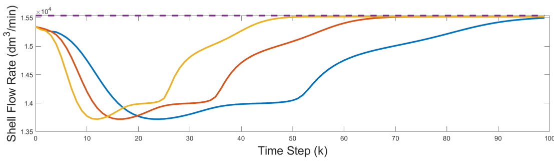

(d) Manipulated variable: inlet volumetric flow rate in shell side

Fig. 4. Effects of tuning parameter on the rate of convergence to steady state

The final scenario explored in this case study is the time-varying disturbance rejection operation. Specifically, the inlet methane concentration within the feed natural gas stream undergoes random fluctuations around 5% of its nominal value. The simulation results, which compare to a disturbance-free steady-state optimal condition, are presented in Figure 5.

The simulation results lead to a primary observation that the closed-loop DMA-MR with noisy inputs does not achieve asymptotic convergence to a steady state. This phenomenon arises from the inherent behavior of self-stabilizing eNMPC, which actively tracks the optimality

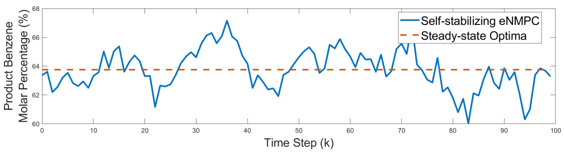

(a) Output variable: benzene molar percentage in retentate

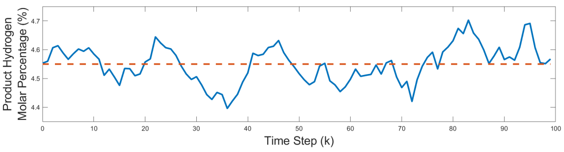

(b) Output variable: hydrogen molar percentage in permeate

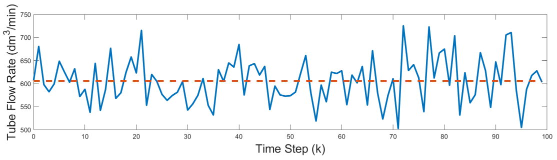

(c) Manipulated variable: inlet volumetric flow rate in tube side

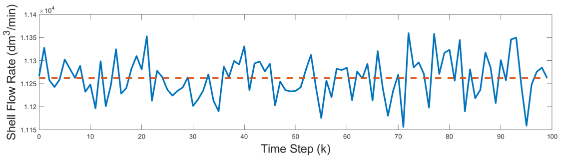

(d) Manipulated variable: inlet volumetric flow rate in shell side

Fig. 5. Self-stabilizing eNMPC with time-varying disturbances

conditions. These conditions, however, undergo changes with each new set of boundary conditions introduced at every time step by time-varying disturbances. Consequently, the self-stabilizing eNMPC effectively converges towards a dynamically shifting target, rendering it incapable of attaining a steady state. Nevertheless, the closed-loop behavior of the eNMPC applied to the DMA-MR system remains bounded rather than becoming unstable. This resilience can be attributed to the inherent input to state practical stability (ISpS) of the previously proposed formulation, even as the new Lyapunov constraint is further tightened through an additional tuning parameter. Additional eNMPC results for the DMA-MR process can be found in Dinh et al. (2024).

5. CONCLUSION

This study explores the practical use of self-stabilizing eNMPC without the reliance on predetermined setpoints. This advancement represents a substantial step forward in overcoming the challenges associated with integrating RTO and advanced regulatory controllers, such as MPC. The proposal of a generalized time-domain formulation addresses the inherent differences between the discrete-time nature of control instrumentation and the continuous-time characteristics of first-principle models. Furthermore, the dynamic adjustment of the Lyapunov constraint's parameters provides operators with enhanced control over the behavior of the closed-loop system, ultimately increasing its adaptability.

A case study examines the implementation and practical performance of self-stabilizing eNMPC in the context of a counter-current DMA-MR system. Various scenarios are explored, providing a unique insight into the operation of the framework. The framework's adaptability to parameter updates showcases its real-time control potential. Tuning parameters significantly influence the membrane system's convergence rates, allowing operators to adjust the control system's response to transient dynamics. Computational efficiency emerged as an advantage, particularly in scenarios without parameter updates. Finally, ISpS is demonstrated in the presence of time-varying disturbances.

ACKNOWLEDGEMENTS

The authors thank the Center for Advanced Process Decision-making at Carnegie Mellon University for providing the funding support for this research.

REFERENCES

Angeli, D., Amrit, R., and Rawlings, J.B. (2012). On Average Performance and Stability of Economic Model Predictive Control. *IEEE Trans. Automat. Contr.*, 57(7), 1615–1626. doi:10.1109/TAC.2011.2179349.

Baldea, M., Edgar, T.F., Stanley, B.L., and Kiss, A.A. (2017). Modular manufacturing processes: Status, challenges, and opportunities. *AIChE Journal*, 63(10), 4262–4272. doi:10.1002/aic.15872.

Bishop, B.A. and Lima, F.V. (2021). Novel Module-Based Design Algorithm for Intensified Membrane Reactor Systems. *Processes*, 9(12), 2165. doi:10.3390/pr9122165.

Dinh, S., Lin, K.H., Lima, F.V., and Biegler, L.T. (2024). Implementation of self-stabilizing economic nonlinear model predictive control to modular systems. *to appear*.

Ladiges, J., Fay, A., Holm, T., Hempen, U., Urbas, L., Obst, M., and Albers, T. (2018). Integration of Modular Process Units Into Process Control Systems. *IEEE Trans. on Ind. Applicat.*, 54(2), 1870–1880. doi:10.1109/TIA.2017.2782679.

Lin, K.H. and Biegler, L.T. (2023). Self-stabilizing economic model predictive control without pre-calculated steady-state optima: Stability and robustness. *Computers & Chemical Engineering*, 178, 108349. doi:10.1016/j.compchemeng.2023.108349.

Nocedal, J. and Wright, S.J. (2006). *Numerical Optimization*. Springer Series in Operation Research and Financial Engineering. Springer, New York, NY, second edition edition.

Parker, R.B., Nicholson, B.L., Siirola, J.D., and Biegler, L.T. (2023). Reshaping block-hierarchical pyomo models for dynamic optimization applications. *Journal of Process Control*, 132, 103–113.

Rawlings, J.B., Mayne, D.Q., and Diehl, M. (2020). *Model Predictive Control: Theory, Computation, and Design*. Nob Hill Publishing, Santa Barbara, California, 2nd edition edition.